Narrow-band imaging pattern classification in oral cavity

Giancarlo Tirelli | Alberto Vito Marcuzzo | Francesca Boscolo Nata

ENT Clinic, Head and Neck Department, Azienda Sanitaria Universitaria Integrata di Trieste, Trieste, Italy

Correspondence
Francesca Boscolo Nata, ENT Clinic, Head and Neck Department, Azienda Sanitaria Universitaria Integrata di Trieste, Strada di Fiume 447, 34149 Trieste, Italy.
Email: francesca.boscolonata@gmail.com

Abstract

Objective: Narrow-band imaging is widely used in the diagnostic work-up of oral lesions. Different oral subsites present three epithelial types (1, 2a and 2b), each with a different structure and function. The aim of this study was to analyse and describe the different vascular patterns seen on narrow-band imaging according to oral epithelial type and histology.

Materials and Methods: The narrow-band imaging photographs of healthy, dysplastic and neoplastic oral mucosa were retrospectively reviewed and divided according to epithelial type and histology. The different narrow-band imaging patterns were analysed, related to the clinical appearance of the specific area, accurately described and drawn by a professional designer.

Results: The photographs of 302 patients were considered. Six patterns were identified: Normal mucosa exhibited different appearance in each type of epithelium; dysplastic mucosa presented the same pattern in type 1 and 2a epithelia, which differed from that of type 2b epithelium; in cancer, mucosal appearance was identical irrespective of epithelial type, due to complete vascular destruction.

Conclusions: The proposed classification could serve as a guide for clinicians approaching narrowband imaging, especially at early stages of the learning curve, to differentiate normal mucosa from malignant lesions and possibly reduce the number of unnecessary biopsies.

KEYWORDS
early diagnosis, narrowband imaging, oral cancer, oral diagnosis, oral mucosa, precancerous conditions

1 | INTRODUCTION

Oral cancer and oropharyngeal cancer together represent the tenth most common cancer worldwide (Cosway, Drinnan, & Paleri, 2016). The estimated new cases for 2018 in the United States are 51,540, with 10,030 related deaths (Siegel, Miller, & Jemal, 2018), with a continuously increasing trend. An early diagnosis could increase the number of survivors, as predicted in a recent paper (Miller et al., 2016). Unfortunately, most oral and oropharyngeal cancers continue to be diagnosed at an advanced stage, requiring extensive surgical approaches or nonsurgical treatments such as radiotherapy (RT) or chemotherapy (CT), which impair function and negatively affect patients' quality of life (Rathod, Livergant, Klein, Witterick, & Ringash, 2015).

During carcinogenesis, vascular structure and architecture undergo considerable changes (Kumagai, Toi, & Inoue, 2002), and these phenomena occur so early as to be already present when the mucosa still appears normal at conventional oral examination. The possibility to diagnose tumours based on angiogenic or vascular morphologic changes might be ideal for the early detection of neoplasm (Muto, Katada, Sano, & Yoshida, 2005), both for primary tumours and for local recurrences or second primaries. The introduction of optical technologies allowing identification

of vascular abnormalities could help to detect cancers at an early stage. Among these technologies, narrow-band imaging (NBI) has widely demonstrated its ability to reveal early mucosal lesions (Ni & Wang, 2016). This optical image-enhanced endoscopy is based on the use of light filters. Two specific wavelengths, 415 and 540 nm, are employed because they can specifically highlight the intrapapillary capillary loop (IPCL) in the superficial mucosa and the thicker blood vessels in the deeper mucosa and submucosa, given that the depth of light penetration in tissue is directly related to wavelength (Gono et al., 2004).

Different IPCL patterns have been described in the various fields of NBI application. After Inoue et al. (2000) first described IPCL patterns in the oesophagus, Watanabe et al. (2009) and Piazza et al. (Piazza, Cocco, De Benedetto, Del Bon, et al., 2010) presented the typical NBI features of laryngeal carcinoma, and Ni et al. (2011) proposed the first classification of IPCLs in precancerous and malignant laryngeal lesions, followed by the more simplistic approach of the European Laryngological Society (Arens et al., 2016). The same was also done by Wen et al. (2012) for the nasopharynx, Fujii et al. (Fujii, Yamazaki, Muto, and Ochiai ,2010) for the oropharynx and Takano et al. (2010) for the oral cavity.

All of the above classifications of vascular appearance, however, are exclusively based on histology and fail to take epithelial structure into consideration. The mucosa of the different regions of the head and neck presents different types of covering epithelium according to the different subsites and their function (Lin, Wang, Lee, Tsai, & Weng, 2012).

The aim of the present study was to provide an accurate description and classification of vascular patterns visible on NBI in the different oral subsites divided according to their epithelial structure, both in normal conditions and in the presence of different grades of dysplasia or carcinoma. We specifically focused on oral subsites (floor of mouth, ventral and dorsal surface of the tongue, labial and buccal mucosa, retromolar trigone and hard palate) because in areas with thick lymphoid tissue, such as the oropharynx, follicular hyperplasia can influence IPCL morphology (Ni & Wang, 2016).

As the oral cavity is generally amenable to visual inspection, we also correlated the NBI results with the clinical appearance of the analysed areas. Even if high-resolution photographs are shown, we decided to provide also the drawings prepared by a professional designer in order to increase the recognition of the more important characteristics and help a less trained eye in their identification.

2 | MATERIALS AND METHODS

This retrospective study was conducted at the ENT Department of Trieste in accordance with the principles stated in the Declaration of Helsinki (1964), and its design was approved by the University of Trieste Ethics Committee (January 16, 2017, Report no. 76).

In July 2016, we searched the hospital department database for all cases of subjects who underwent oral NBI endoscopy between January 2012 and June 2016. These included patients with oral and oropharyngeal cancers undergoing preoperative and intraoperative examinations or postoperative follow-up at our department, and noncancer patients scheduled for a sinonasal or otologic surgery or undergoing audiometric examinations who volunteered to undergo NBI examination. Noncancer patients had no previous or current smoking or drinking habits, nor did they suffer from diabetes mellitus or chronic inflammatory mucosal conditions that could alter the vasculature and introduce a confounding factor (Gong, Wei, Yu, & Pan, 2015; Mauri-Obradors, Estrugi-Devesa, Jané-Salas, Viñas, & López-López, 2017). Each subject undergoing NBI evaluation signed an informed consent form and a privacy policy agreement. Subjects were evaluated by one of the three authors, using a Visera Elite system OTV-S190 videoprocessor and CLV-S190 light source, CH-S190-XZ HDTV (high definition television) camera, OEV261H 26'' LCD HD monitor (Olympus Medical Systems Corp, Tokyo, Japan) with rigid endoscopes with a viewing angle of 0° and 70°. Topical anaesthesia with lidocaine spray 10 g/100 ml was used only if necessary to reduce discomfort. If mobile dental prostheses were present, the subject was asked to remove them before the examination. Irrespective of the reason for performing NBI, a complete assessment of the oral mucosa was carried out in each subject, maintaining the endoscope at a distance of 1 cm or, to avoid patient discomfort when approaching posterior subsites, up to 3 cm but using the camera zoom function. During the examination, the system was switched between white light (WL) HDTV and NBI HDTV by pressing a button on the camera. If an NBI-positive area was found, an incisional biopsy was performed; the histological analysis was reported by a single pathologist who was blinded to the results of NBI. Conversely, if NBI did not show vascular changes, biopsy was not performed for ethical reasons but the patient was re-evaluated after 6 and 12 months to confirm his/her negativity in NBI. Photographs of all examinations were recorded and saved on a computer for further evaluation.

All charts and images of cases of NBI-positive and NBI-negative findings in the various oral subsites were reviewed. Patients undergoing oncologic follow-up who had been treated with radiotherapy either alone or in combination with surgery and/or chemotherapy were excluded from the analysis.

Subjects were divided into two groups:

group A: "NBI-positive"
group B: "NBI-negative"

We defined "NBI-positive" subjects who presented with the known alterations of the intrapapillary capillary loop (IPCL), such as dilatation and crossing, elongation and meandering or pattern destruction and angiogenesis (Takano et al., 2010; Yang et al., 2012; Yang, Lee, Chang, Chien, & Chen, 2013), or in the presence of brown dots (Muto et al., 2004; Piazza, Cocco, Bon, et al., 2010) which can underlie histological changes, and with a histological confirmation of different grades of dysplasia and/or carcinoma on biopsy. It is known that mild IPCL alterations (i.e., dilatation and crossing) may also be detected in inflammatory conditions like aphthae, but in these cases, the same type of

	Group A (*n* = 141)	Group B (*n* = 161)	*p*-Value
Sex, *n* (%)			
Male	98 (69.5)	102 (63.4)	0.27
Female	43 (30.5)	59 (36.6)	
Age, year, mean ± *SD* (range)	69 ± 11 (44–89)	67 ± 10 (42–88)	0.11

TABLE 1 Demographic characteristics of NBI-positive (group A) and NBI-negative (group B) subjects

TABLE 2 Distribution of oral lesions in group A according to epithelial type and histology

Epithelial type	*n* (%)
I	14 (13.1)
IIa	58 (54.2)
IIb	35 (32.7)
Histology	
Mild dysplasia	5 (4.7)
Moderate dysplasia	14 (13.1)
Severe dysplasia	14 (13.1)
Carcinoma	74 (69.1)

IPCL will also be seen surrounding the lesion, which is plastic and painful, thus helping the clinician in the diagnosis: Consequently, we did not consider these lesions as NBI-positive and, if found, we excluded them. To avoid variability in the interpretation of dysplasia, all the biopsies were analysed by a dedicated pathologist. When these vascular alterations were not present, even at the following 6- and 12-month controls, subjects were classified as "NBI-negative".

Because different subsites of the oral mucosa present different epithelial types in terms of thickness and keratinization based on their function, we divided the photographs obtained in each group according to Lin et al.'s classification (Lin et al., 2012): type 1, keratinized thick stratified squamous epithelium which is present in gingiva, hard palate and dorsal surface of the tongue; type 2a, non-keratinized thin stratified squamous epithelium found in the floor of mouth and ventral tongue; type 2b, non-keratinized very thick stratified squamous epithelium of the retromolar trigone, labial and buccal mucosa.

The photographs of each oral subsite in group A were divided according to histological results (mild, moderate, severe dysplasia and carcinoma), and the vascular patterns on NBI were analysed and described to verify whether a specific histology was associated with a constant vascular pattern in a particular subsite.

The photographs of each oral subsite in group B allowed us to describe normal NBI vascular patterns. The judgement of normalcy of the patterns was based on reproducibility of the NBI findings in the same subsite across different patients owing to the ethical implications and feasibility of random biopsy sampling in every patient with negative clinical results.

All the photographs were meticulously studied by the three authors independently, all with at least three years' experience in NBI use, and the microvascular organization (regular, irregular) and appearance of the vascular pattern were accurately described: results were categorized according to the agreement of at least two of three examiners and drawn by a professional designer.

3 | RESULTS

The photographs of 302 subjects were retrospectively reviewed. The demographic characteristics of subjects in the two groups are shown in Table 1. The two groups ("NBI-positive" and "NBI-negative") were comparable in terms of patients' sex and mean age (p = NS).

Among the 141 patients in group A, 107 oral lesions were biopsied: their distribution according to epithelial type and histology is presented in Table 2. None of the lesions was clinically indicative for an inflammatory condition, and consequently, no patients were excluded from the analysis.

At conventional oral endoscopy, the normal mucosa appeared as plane and without evident dyschromic areas, dysplastic lesions appeared as ulcerations (#2), leukoplakia (#12; five flat, two verrucous, five elevated), erythroplakia (#7; four flat, three elevated), flat leukoerythroplakia (#8) or were not visible in four cases, while invasive cancers appeared as ulcerated (#37), vegetating (#20) and flat (#17) lesions. In the "NBI-negative" group, 19 patients wore dentures: they usually presented symmetrical hyperkeratosis in the gingival mucosa were the dentures lay, and none of them presented confounding stomatitis in the denture-bearing areas. We noted that the presence of frictional keratosis along the occlusal line of the cheek mucosa was independent from the use of dentures (p = 0.29) and easily recognizable by its constant position and characteristics (cord-like).

Considering epithelial structure in the different oral subsites and the different histologies, we identified six vascular patterns on NBI.

All normal mucosa presented a "normal" pattern which differed according to the specific subsite (1, 2a and 2b). Its appearance in detail was as follows:

Normal 1: The normal mucosa in subsites covered by type 1 epithelium (gingiva, hard palate and dorsal surface of the tongue) presented thin dark green/brown vessels with small branches arising at an acute angle, which represented the superficial mucosal capillaries. In the posterior hard palate, some of the branching vessels ended with a "flower-like" configuration with a thin vessel acting as a "stem" and several points all around as the "petals", attributable to minor salivary glands. Some large light blue vessels

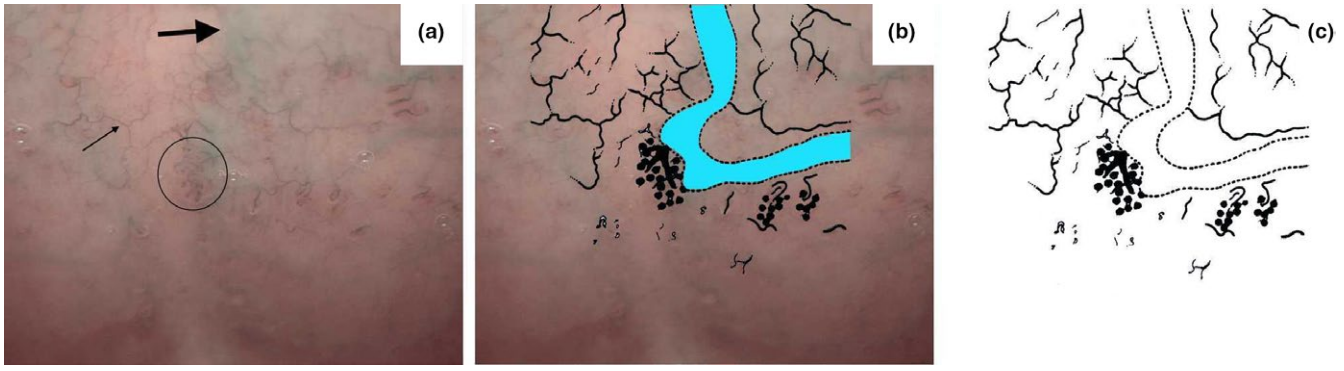

FIGURE 1 Normal pattern in type 1 epithelium. (a) Posterior hard palate appearance on NBI endoscopy. Thin dark green/brown vessels with small branches arising at an acute angle and representing the superficial mucosal capillaries are visible (thin arrow). Some of those branching vessels end with a "flower-like" configuration (circle) with a thin vessel acting as a "stem" and some points all around as the "petals", attributable to minor salivary glands. Some large light blue vessels representing the submucosal veins can be glimpsed (thick arrow). (b) Superficial mucosal capillaries, submucosal veins (in cyan) and flower-like structures are underlined. (c) Schematic representation of the main characteristics of the pattern [Colour figure can be viewed at wileyonlinelibrary.com]

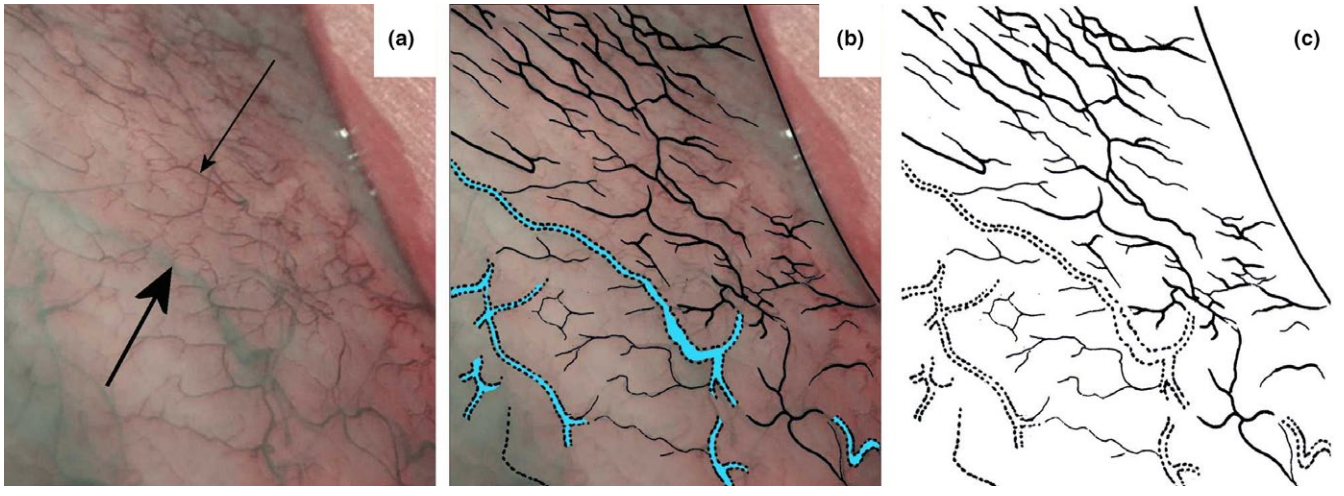

FIGURE 2 Normal pattern in type 2a epithelium. (a) Floor of mouth appearance on NBI endoscopy. Thin dark green/brown parallel vessels with small branches arising at an acute angle and representing the superficial mucosal capillaries are visible (thin arrow). The large light blue vessels representing the submucosal veins are clearly visible (thick arrow). (b) Superficial mucosal capillaries and submucosal veins (in cyan) are underlined. (c) Schematic representation of the main characteristics of the pattern [Colour figure can be viewed at wileyonlinelibrary.com]

representing the submucosal veins could be glimpsed (Figure 1). In the anterior–lateral part of the hard palate and in the mucosa of gingiva, the grade of keratinization is higher and consequently only the superficial capillaries were visible and appeared as punctuations along the palatine crests. The structure of the dorsal surface of the tongue prevented visualization of the NBI pattern.

Normal 2a: The normal mucosa in subsites covered by type 2a epithelium (floor of mouth and ventral tongue) presented thin dark green/brown parallel vessels with small branches arising at an acute angle, which represented the superficial mucosal capillaries. The large light blue vessels representing the submucosal veins were clearly visible (Figure 2).

Normal 2b: The normal mucosa in subsites covered by type 2b epithelium (retromolar trigone, labial and buccal mucosa) presented regular and equidistant dark green/brown small punctuations or short dashes if the vessels were visualized perpendicularly, or thin parallel vessels if they were longitudinal to the mucosa. Some large light blue vessels representing the submucosal veins could be glimpsed (Figure 3).

Preneoplastic lesions presented mild alterations of the vascular pattern ("dysplastic" pattern), which were similar in subsites 1 and 2a, but different in subsite 2b. The presence of leukoplakia or leukoerythroplakia within the lesion (20 cases) prevented visualization of the vascular pattern; in these situations, the pattern could be identified in the surrounding mucosa where the white patch was thinner or not present. None of the dysplastic lesions displayed a "neoplastic" pattern, nor did any of the lesions with a dysplastic pattern present carcinoma at histology.

Dysplastic 1–2a: The mucosa presenting different grades of dysplasia (mild, moderate and severe) at histology appeared as a well-demarcated brownish/purple area with thick dark spots. In the brownish/purple area, the submucosal large light blue vessels were

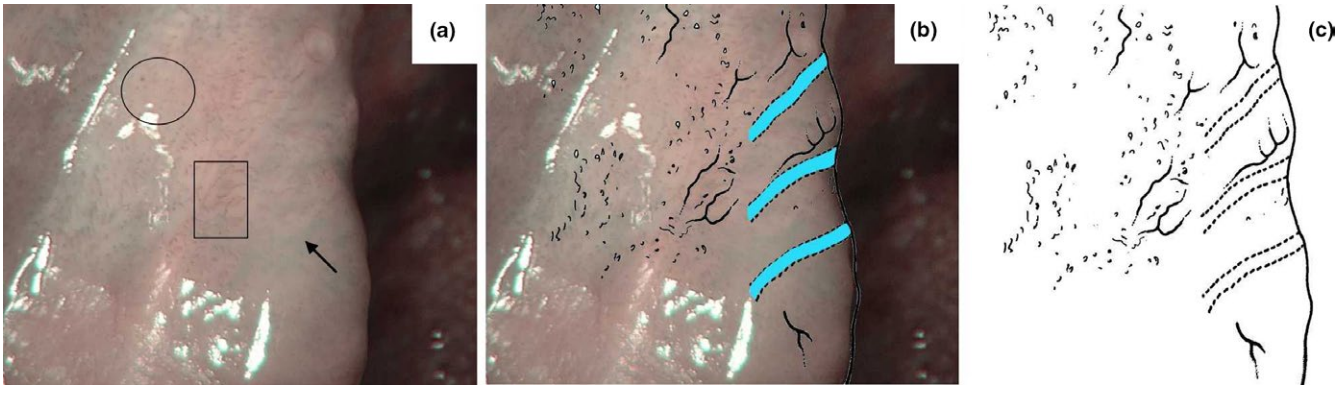

FIGURE 3 Normal pattern in type 2b epithelium. (a) Inferior trigone appearance on NBI endoscopy. Superficial mucosal capillaries are visible as regular and equidistant dark green/brown small punctuations or short dashes (circle) if the vessels are visualized perpendicularly, or as thin parallel vessels (rectangle) if they are longitudinal to the mucosa. Some large light blue vessels representing the submucosal veins can be glimpsed (arrow). (b) Superficial mucosal capillaries and submucosal veins (in cyan) are underlined. (c) Schematic representation of the main characteristics of the pattern [Colour figure can be viewed at wileyonlinelibrary.com]

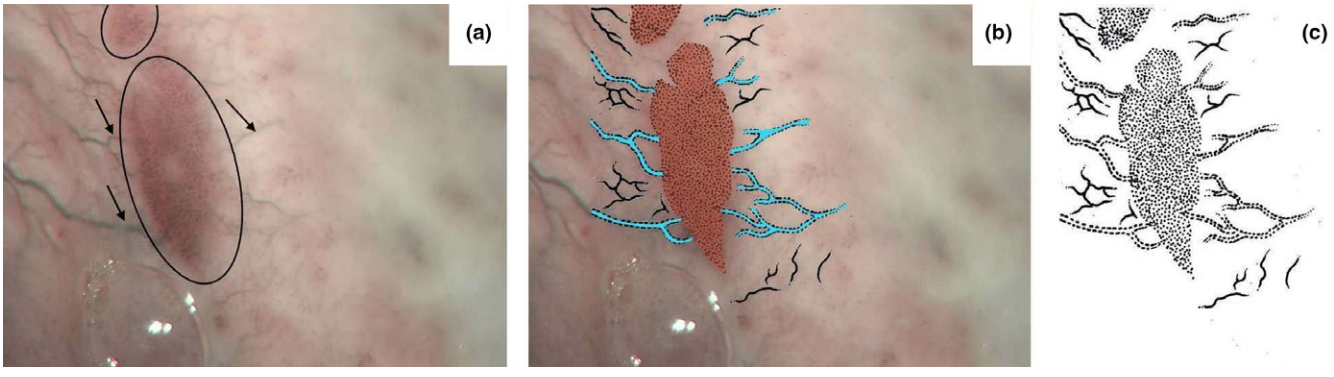

FIGURE 4 Dysplastic pattern in type 1 epithelium. (a) Appearance of a severe dysplasia of the hard palate on NBI endoscopy. A well-demarcated brownish/purple area with thick dark spots is visible (circle); it is perpendicularly reached by dilated light blue vessels (arrows). In the brownish/purple area, the submucosal large light blue vessels are no longer visible. (b) The well-demarcated brownish/purple area perpendicularly reached by dilated light blue vessels (in cyan) is underlined. (c) Schematic representation of the main characteristics of the pattern [Colour figure can be viewed at wileyonlinelibrary.com]

no longer visible. This well-demarcated area was perpendicularly reached by dilated light blue vessels in both type 1 and 2a epithelia (Figures 4 and 5).

Dysplastic 2b: The mucosa presenting different grades of dysplasia (mild, moderate or severe) at histology in type 2b epithelium appeared as a honeycomb mesh made up of multiple polygonal areas representing the dilated superficial vessels. The dysplastic area was less defined because the brownish/purple area was not visible. The submucosal large light blue vessels were no longer visible in the dysplastic area but could sometimes be glimpsed in the surrounding areas (Figure 6).

All cancerous lesions presented the same destruction of the vascular pattern irrespective of the lesion subsite. The only difference was related to the macroscopic appearance of the lesion, described in detail as follows:

Neoplastic: In the case of ulcerated lesions (#37), the presence of a necrotic core prevented visualization of the vasculature although this was visible at the tumour boundaries as dark green spots, dilated winding vessels or as a bobby pin (Figure 7); in the case of vegetating (#20) or flat (#17) lesions, the same vascular appearance could be seen over the whole cancer surface (Figure 8). These unstructured vessels represented the remnants of IPCL.

4 | DISCUSSION

Traditionally, ENT doctors have used clinical examination with white light endoscopy to identify oral and oropharyngeal squamous cell carcinoma (Davies et al., 2015), but premalignant lesions (dysplasia) are often overlooked with this procedure. Optical technologies, using different wavelengths of light to examine suspicious tissue, provide a noninvasive method to guarantee an early diagnosis. Among them, narrowband imaging (NBI), first introduced in gastrointestinal endoscopy (Vu & Farah, 2014), has rapidly extended its field of application to otolaryngology.

Many studies have demonstrated the effectiveness of NBI in the detection of upper aerodigestive tract cancers. However, as underlined in a recent review (Cosway et al., 2016), adequate classifications

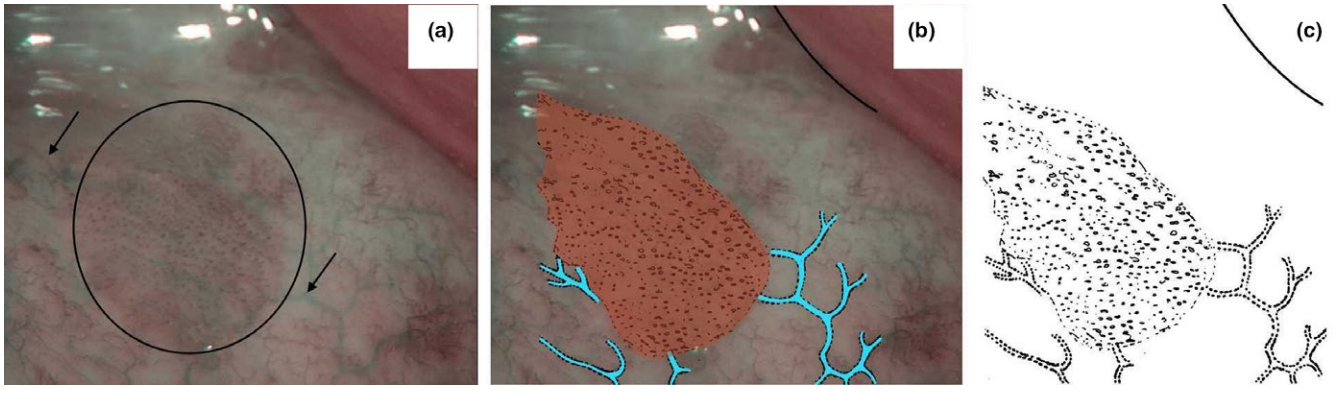

FIGURE 5 Dysplastic pattern in type 2a epithelium. (a) Appearance of a severe dysplasia of the floor of mouth on NBI endoscopy. A well-demarcated brownish/purple area with thick dark spots is visible (circle); it is perpendicularly reached by dilated light blue vessels (arrows). In the brownish/purple area, the submucosal large light blue vessels are no longer visible. (b) The well-demarcated brownish/purple area perpendicularly reached by dilated light blue vessels (in cyan) is underlined. (c) Schematic representation of the main characteristics of the pattern [Colour figure can be viewed at wileyonlinelibrary.com]

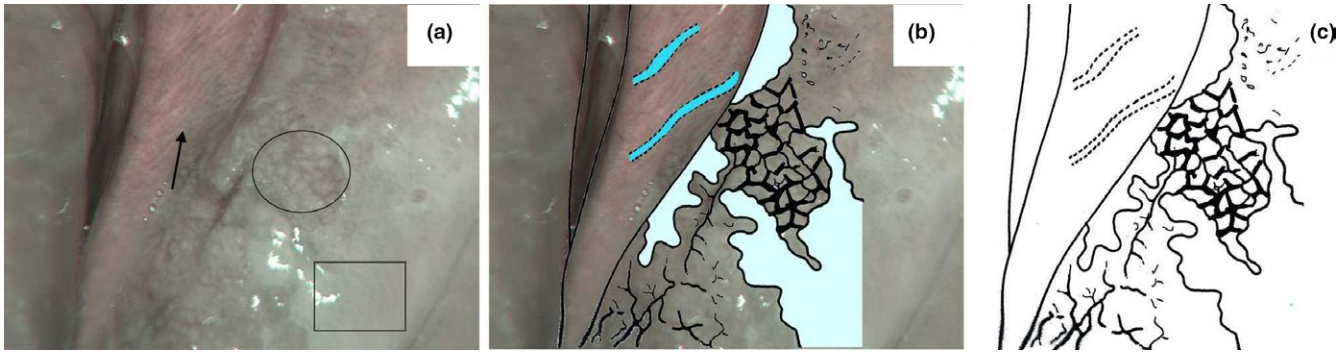

FIGURE 6 Dysplastic pattern in type 2b epithelium. (a) Appearance of a severe dysplasia of an inferior trigone on NBI endoscopy. The image resembles a honeycomb mesh made up of multiple polygonal areas representing the dilated superficial vessels (circle). The dysplastic area is less well defined because the brownish/purple area is not visible. If leukoplakia is present in the context of the lesion, the vascular pattern is not visible beneath it (rectangle). The submucosal large light blue vessels are no longer visible in the dysplastic area but can sometimes be glimpsed in the surrounding areas (arrow). (b) The image resembles a mesh, leukoplakia and the submucosal vessels (in cyan) are underlined. (c) Schematic representation of the main characteristics of the pattern [Colour figure can be viewed at wileyonlinelibrary.com]

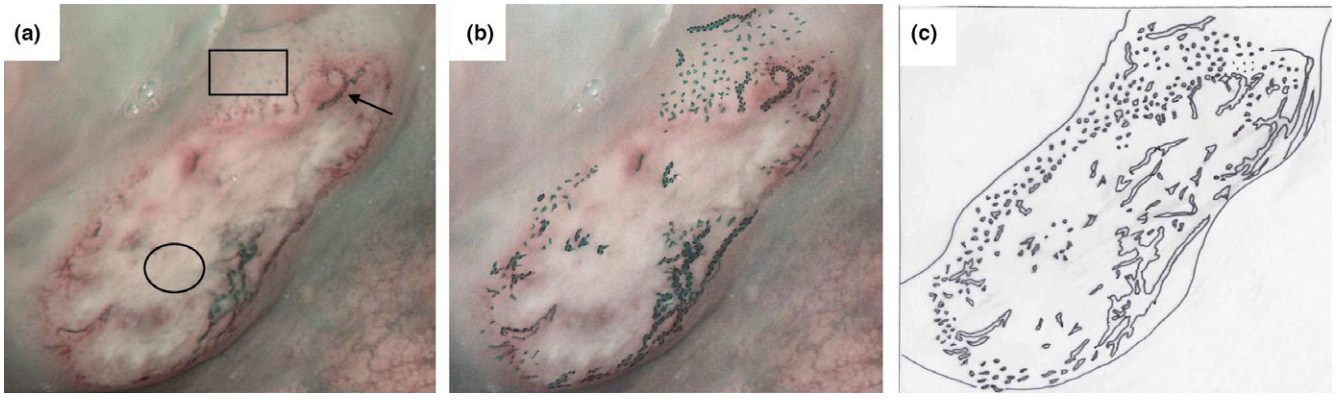

FIGURE 7 Neoplastic pattern in an ulcerated cancerous lesion. (a) Ulcerated cancer of the hard palate on NBI endoscopy. The presence of necrosis in the centre of the lesion prevents visualization of the vasculature (circle) which is, however, appreciable at the tumour limits as dark green spots (rectangle), dilated winding vessels or as bobby pin (arrow), representing IPCL remnants. (b) Dark green spots, dilated winding vessels or bobby pin are underlined. (c) Schematic representation of the main characteristics of the pattern [Colour figure can be viewed at wileyonlinelibrary.com]

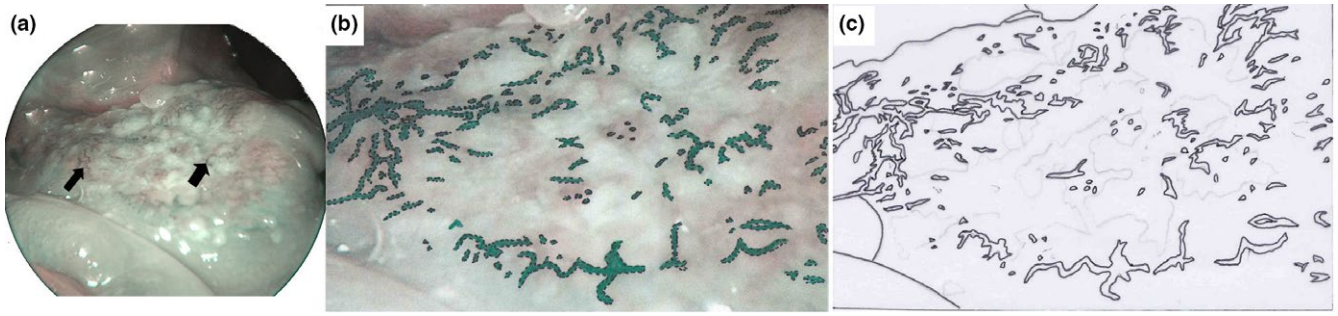

FIGURE 8 Neoplastic pattern in a vegetating cancerous lesion. (a) Vegetating cancer of the floor of mouth on NBI. Unstructured vessels representing the remnants of IPCL and appearing as dark green spots, dilated winding vessels or as bobby pin (arrow) are visible over the whole cancer surface. (b) Dark green spots, dilated winding vessels or bobby pin are underlined. (c) Schematic representation of the main characteristics of the pattern [Colour figure can be viewed at wileyonlinelibrary.com]

of neoplastic and non-neoplastic lesions on NBI have been lacking. The presence of a well-defined brownish area with scattered brown spots (Muto et al., 2004; Piazza, Cocco, De Benedetto, Del Bon, et al., 2010) was the first finding to be considered positive on NBI, but it was strictly dependent on subjective interpretation and the examiner's experience. The introduction of specific vascular pattern classes (Arens et al., 2016; Fujii et al., 2010; Ni et al., 2011; Takano et al., 2010; Wen et al., 2012) allowed different examiners to adhere to a reference classification and avoid ambiguities. The previous classifications were widely accepted because they were shown to have good concordance with histology (Šifrer et al., 2018).

Unlike the mucosa of the other upper aerodigestive tracts, the oral mucosa is unique in that different subsites have specific structure according to function (Nanci, 2013). A previous study describing NBI vascular patterns in the oral cavity (Takano et al., 2010) differentiated the patterns on the basis of histology alone. Conversely, we believe that a complete description of both normal and altered vascular patterns on NBI must also take into account the different epithelial structure.

Oral mucosa is formed by two different components: a covering epithelium and underlying connective tissue called the lamina propria. There are connectival papillae, interdigitating with epithelial ridges, lying between them. This structure guarantees the best metabolic exchange between connectival blood vessels (intrapapillary capillary loops [IPCL]) and the overlying avascular epithelium. IPCLs are more represented in the upper part of the lamina propria, called the superficial papillary layer (Nanci, 2013). It is these IPCLs that are identified by NBI, which therefore empowers clinicians to reach an early diagnosis of mucosal lesions. Indeed, as underlined in a systematic review, there is a direct relation between the IPCL pattern visualized with NBI and histology: as the IPCL pattern changes from I to IV, histological severity increases. In detail, the upward extension of IPCL proceeds in accordance with the degree of dysplasia (Vu & Farah, 2014).

As previously stated, the mucosa of each oral subsite is different because of its anatomical and functional characteristics. Lin et al. (2012) hypothesized that NBI differed in its ability to identify IPCL according to epithelial structure, but Piazza et al. (2016) recently denied this view. They underlined the difference between the epithelial thickness (i.e., from the epithelial surface to the basal membrane) and the depth of penetration needed to assess IPCL patterns (i.e., from the mucosal surface to the papillary apex). Because the length of the papillae increases according to epithelial thickness, the distance between the mucosal surface and the papillary apex always remains within the limit of NBI wavelength penetration: consequently, NBI can highlight IPCL in all types of epithelium.

In our experience, we were able to identify IPCL in all three types of oral epithelium, both in normal and in dysplastic or neoplastic histology, which confirms that NBI performance is not limited by epithelial structure. Moreover, Piazza et al. (2016) underlined how tumour-induced neoangiogenesis produces elongation of IPCLs and formation of intraepithelial vessels that are not present in normal mucosa. This may account for our finding that IPCLs in the hard palate were less visible in normal mucosa because of its thickness and keratinization, but they became much more evident in dysplastic lesions where they appeared as thick dark spots perpendicularly reached by dilated light blue vessels, because of the development of new IPCLs in the superficial mucosal layer.

We found the influence of epithelial structure on NBI visualization of IPCL to be especially evident in normal mucosa. In fact, the vascular network, both superficial and deep, was readily visible in thin type 2a epithelium, while its identification was more difficult in subsites with thicker type 1 and 2b epithelium. Although these differences may appear barely appreciable to an untrained eye, in our opinion it is fundamental to learn to recognize them because they allow one to understand the modifications occurring during carcinogenesis. For example, if submucosal veins, which are normally well defined in type 2a epithelium, start to disappear and thick dark spots appear in a well-defined area, this may alert the clinician to the presence of histological alterations.

The difference according to subsite became less evident in the case of histological alterations because during carcinogenesis IPCLs undergo many changes in number and calibre and upward shifting irrespective of the specific epithelial structure (Kumagai et al., 2002). The dilatation and elongation of IPCLs during transformation from normal epithelium to cancer was visualized in our

experience as thick dark dots in a brown/purple well-defined area (dysplastic 1 and 2a) or as a mesh-like image (dysplastic 2b). The presence of a mucosa firmly attached to the underlying structures in subsites with type 2b epithelium, or the different orientation of IPCLs, perpendicular or longitudinal to the mucosa, could explain the different vascular patterns observed in the case of dysplasia in our series. The same histological alteration (dysplasia) was in fact more evident in subsites with type 1 and 2a epithelia and less in the thicker type 2b epithelium. A clinician should take this finding into account because it is possible that vascular alterations in type 2b epithelium become visible later than in the other subsites. Kumagai et al. (2002) stated that during the mucosal transformation the arborescent vascular network becomes less transparent than normal mucosa; this was confirmed in our experience by the fact that submucosal veins, which appeared as large light blue vessels (more or less visible according to epithelial thickness), were no longer visible in the case of dysplasia in all three types of epithelium.

We did not find differences in the vascular pattern according to grade of dysplasia (mild, moderate, severe) in any of the three types of epithelium. The different grades of dysplasia (Gale et al., 2005) are classified based on the level of the epithelium in which architectural disruption can be found at microscopic evaluation and therefore cannot be appreciated on superficial inspection of the mucosa with NBI, justifying our observations. Moreover, it should be emphasized that NBI cannot replace histological assessment, but can only indicate which lesions should be biopsied and which can be followed up, reducing the number of unnecessary biopsies. The present study does not intend to provide a rigid classification correlating vascular changes and histology, especially in the case of the different grades of dysplasia.

As described by Kumagai et al. (2002), IPCLs and the pre-existing vasculature are lost in invasive cancers and replaced by a tumour neovasculature, which is leaky and has an irregularly shaped fragile structure. Our series confirmed this observation and verified the influence of the macroscopic tumour appearance. In invasive cancers appearing as ulcerating lesions with a necrotic core, the vascular networks were no longer visible, although the IPCL remnants appeared as short winding dark green lines along the tumour limits. In the case of flat or vegetating lesions, these destroyed IPCLs were visible over the whole tumour surface.

We found two situations preventing the evaluation of vascularization on NBI: the presence of necrotic tissue and the presence of thick white patches. These observations had already been reported by previous studies (Ni & Wang, 2016; Yang et al., 2013).

In the case of necrosis, the vessels are completely destroyed and the vascular pattern is no longer visible. We think this problem is of secondary importance because ulcerated lesions with a necrotic core are readily identifiable as neoplastic even on conventional oral examination; however, in case of doubt, the presence of dark green spots, dilated winding vessels or bobby pin at the tumour boundaries on NBI can guide the diagnosis.

The strength of NBI lies in its ability to allow an early diagnosis of lesions that are not otherwise visible. The majority of cases of leukoplakia do not progress to cancer and may regress (Gale et al., 2005); on the other hand, the presence of dysplasia in oral leukoplakia is associated with a high risk of progression to cancer (Yang et al., 2013). As a consequence, it is very important to distinguish between the lesions to be biopsied and the ones to be followed up. Conventional oral examination could be limited in this respect because sometimes oral dysplasia might not display specific characteristics. Conversely, the clinician may find NBI to be helpful: although NBI is unable to assess the vascular pattern under a thick white patch because of the "umbrella effect" (Arens, Betz, Kraft, & Voigt-Zimmermann, 2017), evaluation of surrounding areas or where the patch is thinner could be suggestive of the mucosal histology under the leukoplakia (Takano et al., 2010; Yang et al., 2012). In our experience, 20 lesions appeared as leukoplakia or leukoerythroplakia on conventional oral examination; NBI analysis of the surrounding mucosa allowed us to identify a dysplastic pattern and prompted a biopsy which found 4 mild, 8 moderate and 8 severe dysplasia, consistent with previous reports.

Although a trained eye should be able to discern typical postradiotherapy vascular changes (Piazza, Cocco, Benedetto, Bon, et al., 2010) after a learning curve of at least 6 months (Tirelli et al., 2017), in the present study we decided to exclude patients previously treated with radiotherapy so as to avoid bias. Future studies specifically focused on these patients are necessary to understand whether the vascular changes related to previous radiotherapy appear different according to the oral subsite and whether they show different patterns when dysplasia and cancer develop. Other areas of future research include the analysis of vascular patterns in the case of trauma and inflammation in the different oral subsites, and the description of NBI vascular patterns also in the oropharynx to assess the effect of lymphoid tissue.

In conclusion, the identification of altered vascular patterns assumes knowledge of what can be considered "normal", especially because the presence of different types of epithelium in oral subsites can further complicate the interpretation of the vascular pattern. The present study aimed to investigate the NBI appearance of microvascular characteristics according to the different oral subsites and histologies.

Any classification should have clinical relevance. We believe our classification fulfils this requirement in that it can simplify the differentiation between normal epithelium and malignant (dysplastic and cancerous) lesions and help identify the lesions to be biopsied. Although histological examination after formalin embedding clearly remains the gold standard to define the nature of the lesion, we believe NBI could help both to reduce unnecessary biopsies and ensure that potentially dangerous lesions are not overlooked. Future prospective studies are required to validate the proposed classification and confirm the close correlation between NBI appearance and histology in the different oral subsites.

We hope the classification presented with photographs and drawings can serve as a guide for clinicians approaching NBI technology and reduce interobserver variability in image interpretation. It is clearly not meant to replace constant training, which is a prerequisite for acquiring confidence with NBI, but could represent a help in overcoming the steep learning curve.

ACKNOWLEDGEMENTS

The authors thank Itala Mary Ann Brancaleone, MA, RSA Dip TEFLA, teacher of Medical English at the University of Trieste, for her support in editing the manuscript. The authors thank Laura Zicari and Fabrizio Rovelli for technical help in drawing the figures.

CONFLICTS OF INTEREST

None to declare.

AUTHOR CONTRIBUTIONS

Giancarlo Tirelli designed the study, analysed data and finally revised the manuscript Alberto Vito Marcuzzo analysed data and drafted the manuscript Francesca Boscolo Nata analysed data and drafted the manuscript

ORCID

Francesca Boscolo Nata http://orcid.org/0000-0003-0758-2376

REFERENCES

Arens, C., Betz, C., Kraft, M., & Voigt-Zimmermann, S. (2017). Narrow band imaging for early diagnosis of epithelial dysplasia and microinvasive tumors in the upper aerodigestive tract. *HNO*, *65*(Suppl 1), 5–12. https://doi.org/10.1007/s00106-016-0284-x.

Arens, C., Piazza, C., Andrea, M., Dikkers, F. G., Tjon Pian Gi, R. E., Voigt-Zimmermann, S., & Peretti, G. (2016). Proposal for a descriptive guideline of vascular changes in lesions of the vocal folds by the committee on endoscopic laryngeal imaging of the European Laryngological Society. *European Archives of Otorhinolaryngology*, *273*, 1207–1214. https://doi.org/10.1007/s00405-015-3851-y.

Cosway, B., Drinnan, M., & Paleri, V. (2016). Narrow band imaging for the diagnosis of head and neck squamous cell carcinoma: A systematic review. *Head and Neck*, *38* (Suppl. 1), E2358–E2367. https://doi.org/10.1002/hed.24300.

Davies, K., Connolly, J. M., Dockery, P., Wheatley, A. M., Olivo, M., & Keogh, I. (2015). Point of care optical diagnostic technologies for the detection of oral and oropharyngeal squamous cell carcinoma. *The Surgeon*, *13*, 321–329. https://doi.org/10.1016/j.surge.2015.06.004.

Fujii, S., Yamazaki, M., Muto, M., & Ochiai, A. (2010). Microvascular irregularities are associated with composition of squamous epithelial lesions and correlate with subepithelial invasion of superficial-type pharyngeal squamous cell carcinoma. *Histopathology*, *56*, 510–522. https://doi.org/10.1111/j.1365-2559.2010.03512.x.

Gale, N., Pilch, B. Z., Sidransky, D., El-Naggar, A. K., Westra, W., Califano, J., … MacDonald, D. G. (2005). *Tumours of the oral cavity and oropharynx (Epithelial precursor lesions). Pathology and genetics of Head and neck tumours* (pp. 177–179). Lyon: IARC Press.

Gong, Y., Wei, B., Yu, L., & Pan, W. (2015). Type 2 diabetes mellitus and risk of oral cancer and precancerous lesions: A meta-analysis of observational studies. *Oral Oncology*, *51*, 332–340. https://doi.org/10.1016/j.oraloncology.2015.01.003.

Gono, K., Obi, T., Yamaguchi, M., Ohyama, N., Machida, H., Sano, Y., … Endo, T. (2004). Appearance of enhanced tissue features in narrow-band endoscopic imaging. *Journal of Biomedical Optics*, *9*, 568–577. https://doi.org/10.1117/1.1695563

Inoue, H., Kumagai, Y., Yoshida, T., Kawano, T., Endo, M., & Iwai, T. (2000). High-magnification endoscopic diagnosis of the superficial esophageal cancer. *Digestive Endoscopy*, *12*, S32–S35. https://doi.org/10.1046/j.1443-1661.2000.00053.x.

Kumagai, Y., Toi, M., & Inoue, H. (2002). Dynamism of tumour vasculature in the early phase of cancer progression: Outcomes from oesophageal cancer research. *The Lancet Oncology*, *3*, 604–610. https://doi.org/10.1016/S1470-2045(02)00874-4

Lin, Y. C., Wang, W. H., Lee, K. F., Tsai, W. C., & Weng, H. H. (2012). Value of narrow band imaging endoscopy in early mucosal head and neck cancer. *Head and Neck*, *34*, 1574–1579. https://doi.org/10.1002/hed.21964.

Mauri-Obradors, E., Estrugi-Devesa, A., Jané-Salas, E., Viñas, M., & López-López, J. (2017). Oral manifestations of diabetes mellitus: A systematic review. *Medicina Oral Patología Oral Y Cirugía Bucal*, *22*, e586–e594. https://doi.org/10.4317/medoral.21655.

Miller, K. D., Siegel, R. L., Lin, C. C., Mariotto, A. B., Kramer, J. L., Rowland, J. H., … Jemal, A. (2016). Cancer treatment and survivorship statistics. *CA: A Cancer Journal for Clinicians*, *66*, 271–289. https://doi.org/10.3322/caac.21349.

Muto, M., Katada, C., Sano, Y., & Yoshida, S. (2005). Narrow band imaging: A new diagnostic approach to visualize angiogenesis in superficial neoplasia. *Clinical Gastroenterology and Hepatology*, *3*(Suppl 1), S16–S20. https://doi.org/10.1016/S1542-3565(05)00262-4

Muto, M., Nakane, M., Katada, C., Sano, Y., Ohtsu, A., Esumi, H., … Yoshida, S. (2004). Squamous cell carcinoma in situ at oropharyngeal and hypopharyngeal mucosal sites. *Cancer*, *101*, 1375–1381. https://doi.org/10.1002/cncr.20482

Nanci, A. (2013). *Ten Cate's oral histology development, structure, and function* (8th ed). St. Louis, MO: Elsevier Mosby.

Ni, X. G., He, S., Xu, Z. G., Gao, L., Lu, N., Yuan, Z., … Wang, G. Q. (2011). Endoscopic diagnosis of laryngeal cancer and precancerous lesions by narrow band imaging. *The Journal of Laryngology & Otology: JLO*, *125*, 288–296. https://doi.org/10.1017/S0022215110002033.

Ni, X. G., & Wang, G. Q. (2016). The role of Narrow Band Imaging in head and neck cancers. *Current Oncology Reports*, *18*, 10. https://doi.org/10.1007/s11912-015-0498-1.

Piazza, C., Cocco, D., De Benedetto, L., Bon, F. D., Nicolai, P., & Peretti, G. (2010). Role of narrow-band imaging and high-definition television in the surveillance of head and neck squamous cell cancer after chemo- and/or radiotherapy. *European Archives of Otorhinolaryngology*, *267*, 1423–1428. https://doi.org/10.1007/s00405-010-1236-9.

Piazza, C., Cocco, D., De Benedetto, L., Del Bon, F. D., Nicolai, P., & Peretti, G. (2010). Narrow band imaging and high definition television in the assessment of laryngeal cancer: A prospective study on 279 patients. *European Archives of Otorhinolaryngology*, *267*, 409–414. https://doi.org/10.1007/s00405-009-1121-6.

Piazza, C., Cocco, D., Del Bon, F., Mangili, S., Nicolai, P., Majorana, A., … G. (2010). Narrow band imaging and high definition television in evaluation of oral and oropharyngeal squamous cell cancer: A prospective study. *Oral Oncology*, *46*, 307–310. https://doi.org/10.1016/j.oraloncology.2010.01.020.

Piazza, C., Del Bon, F., Paderno, A., Grazioli, P., Perotti, P., Barbieri, D., … Nicolai, P. (2016). The diagnostic value of narrow band imaging in different oral subsites. *European Archives of Otorhinolaryngology*, *273*, 3347–3353. https://doi.org/10.1007/s00405-016-3925-5.

Rathod, S., Livergant, J., Klein, J., Witterick, I., & Ringash, J. (2015). A systematic review of quality of life in head and neck cancer treated with surgery with or without adjuvant treatment. *Oral Oncology*, *51*, 888–900. https://doi.org/10.1016/j.oraloncology.2015.07.002.

Siegel, R. L., Miller, K. D., & Jemal, A. (2018). Cancer statistics, 2018. *CA: A Cancer Journal for Clinicians*, *68*, 7–30. https://doi.org/10.3322/caac.21442.

Šifrer, R., Rijken, J. A., Leemans, C. R., Eerenstein, S. E. J., van Weert, S., Hendrickx, J. J., … Rinkel, R. N. P. M. (2018). Evaluation of vascular features of vocal cords proposed by the European Laryngological

Society. *European Archives of Otorhinolaryngology*, *275*, 147–151. https://doi.org/10.1007/s00405-017-4791-5.

Takano, J. H., Yakushiji, T., Kamiyama, I., Nomura, T., Katakura, A., Takano, N., & Shibahara, T. (2010). Detecting early oral cancer: Narrowband imaging system observation of the oral mucosa microvasculature. *International Journal of Oral and Maxillofacial Surgery*, *39*, 208–213. https://doi.org/10.1016/j.ijom.2010.01.007.

Tirelli, G., Piovesana, M., Bonini, P., Gatto, A., Azzarello, G., & Boscolo Nata, F. (2017). Follow-up of oral and oropharyngeal cancer using narrow-band imaging and high-definition television with rigid endoscope to obtain an early diagnosis of second primary tumors: A prospective study. *European Archives of Otorhinolaryngology*, *274*, 2529–2536. https://doi.org/10.1007/s00405-017-4515-x.

Vu, A. N., & Farah, C. S. (2014). Efficacy of narrow band imaging for detection and surveillance of potentially malignant and malignant lesions in the oral cavity and oropharynx: A systematic review. *Oral Oncology*, *50*, 413–420. https://doi.org/10.1016/j.oraloncology.2014.02.002.

Watanabe, A., Taniguchi, M., Tsujie, H., Hosokawa, M., Fujita, M., & Sasaki, S. (2009). The value of narrow band imaging for early detection of laryngeal cancer. *European Archives of Otorhinolaryngology*, *266*, 1017–1023. https://doi.org/10.1007/s00405-008-0835-1.

Wen, Y. H., Zhu, X. L., Lei, W. B., Zeng, Y. H., Sun, Y. Q., & Wen, W. P. (2012). Narrow-band imaging: A novel screening tool for early nasopharyngeal carcinoma. *Archives of Otolaryngology- Head & Neck Surgery*, *138*, 183–188. https://doi.org/10.1001/archoto.2011.1111.

Yang, S. W., Lee, Y. S., Chang, L. C., Chien, H. P., & Chen, T. A. (2013). Light sources used in evaluating oral leukoplakia: Broadband white light versus narrow band imaging. *International Journal of Oral and Maxillofacial Surgery*, *42*, 693–701. https://doi.org/10.1016/j.ijom.2012.10.039.

Yang, S. W., Lee, Y. S., Chang, L. C., Hwang, C. C., Luo, C. M., & Chen, T. A. (2012). Use of endoscopy with narrow-band imaging system in evaluating oral leukoplakia. *Head and Neck*, *34*, 1015–1022. https://doi.org/10.1002/hed.2185.